CORE
Metadata, citation and similar papers at core.ac.uk
Provided by UMP Institutional Repository

ESTIMATION OF THERMAL CONTACT CONDUCTANCE VALUE BETWEEN BORON STEEL BLANK AND TOOL SURFACE AT DIFFERENT VALUE OF APPLIED PRESSURE IN HOT STAMPING PROCESS

MOHD ALI HANAFIAH BIN SHAHARUDIN

Thesis submitted in fulfillment of the requirements
for the award of the degree of
Master of Engineering in Manufacturing

Faculty of Manufacturing Engineering
UNIVERSITI MALAYSIA PAHANG

AUGUST 2014

ABSTRACT

In hot stamping, one of the key factor for successful process control as well as producing a final part strength of more than 1500 MPa is the ability to control heat transfer from the blank throughout the process especially during quenching where the blank need to be cooled down rapidly to transform it's microstructure into martensite phase. In order to control heat transfer process, a study need to be carried out for understanding the characteristics of heat transfer between two solid bodies in contact to each other and investigates the influence of applied pressure to the heat transfer as well as optimizing its. To do so, a systematic approach has been planned to analyze the heat transfer using finite element analysis (FEA) using commercial simulation software as well as the experimental work. The FEA is done by simulating the heated blank or the specimen cool down as it brought into contact to the tools which has a temperature slightly lower than ambient temperature. The effect of different values of applied pressure is simulates by manipulating the values of thermal contact conductance at the blank and tool surface in contact and the thermal contact conductance values will be simulates ranging in between 1000 to 2000 W/m^{2}K. Meanwhile, the experiment being conducted to measure temperature changes of the blank and tool as it is compress in between a set of experimental tool (upper and lower tool) at different pressure ranging between 5 to 35 MPa. The experiment results will be used to compute the actual thermal contact conductance and compared with the FEA simulation. Based on these analyzed result from both approach, the influence of the applied pressure to the heat transfer between two solid bodies in contact as well as the optimum value of applied pressure possibly defined.

ABSTRAK

Dalam proses acuan tekan panas, salah satu faktor utama untuk mengawal proses dengan jayanya serta menghasilkan kekuatan akhir produk lebih daripada 1500 MPa adalah keupayaan untuk mengawal pemindahan haba daripada kepingan asal besi sepanjang proses itu terutama semasa proses lindapkejut dimana kepingan asal besi disejukan semula dengan cepat untuk mengubah mikrostrukturnya kepada fasa martensit. Dalam usaha untuk mengawal proses pemindahan haba, satu kajian perlu dilakukan untuk memahami ciri-ciri pemindahan haba antara dua bahan legap bersentuhan diantara satu sama lain dan menyiasat pengaruh tekanan digunakan untuk pemindahan haba dan juga mengoptimumkannya. Untuk berbuat demikian, pendekatan yang sistematik telah dirancang untuk menganalisis pemindahan haba menggunakan analisis unsur terhingga (FEA) menggunakan perisian simulasi komersil dan juga kerja-kerja uji kaji. FEA itu dilakukan dengan mensimulasi kepingan asal besi atau specimen yang telah dipanaskan menyejuk setelah bersentuhan dengan alat yang mempunyai suhu yang lebih rendah daripada suhu bilik. Manakala perbezaan tekanan di simulasikan dengan memanipulasi nilai-nilai haba kekonduksian sentuhan diantara permukaan kepingan asal besi dan alat ujikaji dan nilai-nilai haba kekonduksian sentuhan akan dimanupulasikan diantara 1000-2000 W/m^{2}K. Sementara itu, eksperimen yang dijalankan untuk mengukur perubahan suhu alat yang kepingan asal besi yang telah dipanaskan dan di tekan diantara alat uji kaji (alat atas dan bawah) pada tekanan yang berbeza antara 5-35 MPa. Keputusan eksperimen akan digunakan untuk mengira kekonduksian sentuhan terma sebenar dan dibandingkan dengan simulasi FEA itu. Berdasarkan keputusan yang dianalisis dari kedua-dua pendekatan, pengaruh tekanan terhadap pemindahan haba antara dua objek legap bersentuhan serta nilai tekanan optimum dapat ditakrifkan.

‘

TABLE OF CONTENTS

	Page
SUPERVISOR'S DECLARATION	ii
STUDENT'S DECLARATION	iii
ACKNOWLEDGEMENTS	iv
ABSTRACT	v
ABSTRAK	vi
TABLE OF CONTENTS	vii
LIST OF TABLES	x
LIST OF FIGURES	xi
LIST OF SYMBOLS	xx
LIST OF ABBREVIATIONS	xxi

CHAPTER 1 INTRODUCTION

1.0	Current Trend		1
1.1	Hot Stamping Process		3
1.2	Problem Statement		5
1.3	Research Objectives		6
1.4	Research Scope		7
1.5	Thesis Arrangement		7

CHAPTER 2 LITERATURE REVIEW

2.0	Introduction		8
2.1	Boron Steel Material		8
	2.1.1	Material Rheology	11
	2.1.2	hardenability	12
	2.1.3	Formability	16
	2.1.4	Coating	17
2.2	Heating Methods		18
2.3	Hot Stamping Process		21

2.3.1 Tailored Die Quench 23
2.3.2 Cutting Operation 28
2.4 Heat Transfer Coefficient 34
2.5 Hot Stamping Tool 37
2.5.1 Tool Materials 39
2.5.2 Tool Cooling System 39
2.6 Summary 41

CHAPTER 3 METHODOLOGY

3.0 Introduction 43
3.1 Finite Element Analysis 46
3.1.1 Tool Design and 3D Model 47
3.1.2 Analysis of Heat Loss During Transferring 49
3.1.3 Analysis of Blank Cooling Inside Tool 52
3.2 Experimental Approach 55
3.2.1 Experimental Setup 57
3.2.2 Experimental Procedure 58
3.2.3 Assumption 59
3.3 Summary 59

CHAPTER 4 HEAT TRANSFER IN HOT STAMPING PROCESS

4.0 Introduction 61
4.1 One Dimensional Heat Diffusion Equation 62
4.2 Numerical Model of Heat Transfer 65
4.3 Heat Transfer At Contact Interface 70
4.4 Summary 72

CHAPTER 5 RESULTS AND DISCUSSIONS

5.0 Introduction 73
5.1 Thermal Analysis Result 73

5.1.1 Result of Heat Loss During Transferring 73
5.1.2 Result of Blank Cooling Inside Tool 76
5.2 Experimental Result 83
5.3 Analysis of Results 89
5.3.1 Validation of Thermal Contact Conductance Values. 94
5.3.2 Analysis Of Blank Cooling Time 102
5.3.3 Actual Blank Cooling Rate 105
5.3.4 Final Hardness 106
5.4 Summary 107

CHAPTER 6 CONCLUSIONS AND SUGGESTION FOR FUTURE WORK

6.0 Introduction 108
6.1 Conclusion 108
6.2 Future Work 109

REFERENCES

APPENDICES

A Table Properties Of Saturated Water
B Calculation Of Flow Rate Of Cooling Fluid
C Calculation Of Heat Convection Coefficient At Cooling Channel
D Simulation Results Data
E Experiment Results Data

LIST OF TABLES

Table No.	Title	Page
2.1	Chemical composition based on weight percentage of boron steel and mechanical properties of boron steel before and after die quenching	9
2.2	Temperature dependent properties of boron steel	11
3.1	Thermal properties of stavax tool steel used in the experiment	49
3.2	Heat convection and radiation coefficient of boron steel (USIBOR 1500) at different temperature	50
3.3	Summary of thermal load and boundary condition in the analysis of heat loss of blank during transferring	51
3.4	Equivalent value of thermal contact conductance at different applied pressure	54
3.5	List of thermal load and boundary condition apply to the analysis of blank cooling inside tool	55
3.6	Equivalent of applied pressure to blank and the hydraulic cylinder pressure	58
5.1	Time study for transferring time and tool closing time in the actual experiment.	84

LIST OF FIGURES

Figure No.	Title	Page
1.1	Yield strength comparison between boron steel (code name: 22mnb5) and typical sheet metal used for automotive component	2
1.2	Typical vehicle component produced from boron steel sheet	3
1.3	Typical process flow of hot stamping process	4
1.4	Continuous cooling transformation diagram of 22MnB5 boron steel	5
2.1	Temperature, time and transformation diagram of boron steel at different cooling rate	10
2.2	Flow behavior of boron steel at different a) temperature b) strain rates.	12
2.3	(a.): Strength comparison between hardened and annealed boron steel (b.): Influence of austenization temperature to the final strength of the boron steel.	13
2.4	Result of tensile test of specimen quench with different cooling rate.	14
2.5	Result of hardness achieved after being quench inside tool at different austenization time and temperature.	15
2.6	(a.):Forming limit diagram based on logan-hosford yield criterion (b.): Forming limit diagram based on iso 12004.	16

2.7 Phase formation of aluminum silicon coating at different austenization temperature 17

2.8 (a.): Roller heart furnace (b.): Induction heating (c.): Resistance heating 19

2.9 (a.): Schematics diagram of the customized induction furnace with conveyor system. (b.): Result of temperature curve over time at different feeding speed. 19

2.10 (a.): Arrangement of the rectangular electrode on sheet. (b.): The temperature distribution on the heated area using thermal camera (c.): temperature gradient curve over input energy and heating time. 20

2.11 (a.): Process flow of hot stamping direct hot stamping (b.): Indirect hot stamping 21

2.12 Range of automotive chassis components produced by hot stamping process 23

2.13 (a.): Combination of two different material properties on b-pillar component using tailored die quench in hot stamping, (b.): Comparison between thermal process control and tailor welded blank. 24

2.14 Comparison between approaches in thermal process control of tailored die quench 25

2.15 (a.): Experimental tool for tailor die quenching using controlled contact surface approach (b.): Controlled tool temperature approach 26

2.16 Specimen shape formed by the experimental tool and result of hardness distribution across the specimen from the center point. 27

2.17 Location of measured point on the specimen and result of hardness variation at different zone and tool temperature 27

2.18 (a.): Shear band condition at different cutting clearance (b.): Cutting force curve over the cutting clearance 29

2.19 Die cutting edge wear condition after a numbers of cutting cycle ranging from 0 to 2000 stroke. 29

2.20 Result of cutting of hardened boron steel at elevated temperature (a.): Effect of cutting temperature to the cutting force (b.): Effect of cutting clearance to the shear band condition 31

2.21 Result of shrinkage effect to final hole dimension at different cutting temperature 32

2.22 Operating sequence of the experimental cutting tool with pair of rectangular electrodes. 33

2.23 (a.): Result of cutting load over the heated zone temperature (b.): Hardness reduction from original value along the x and y-axis from the hole edge 34

2.24 Range of thermal contact conductance values at different contact pressure based on three different experiments. 35

2.25 Thermal contact conductance changes with increasing of tool temperature. 36

2.26 (a.): Experimental approach on determining thermal contact 37 resistance, (b.) Dimensionless thermal contact resistance in function of time

2.27 Comparison between single and double action tool construction in hot stamping process (a.): Single action tool (b.): Double action tool. 38

2.28 Critical criteria of the cooling channel positioning in the hot stamping tool a-cooling holes diameter, b- distance between cooling holes and c-distance to loaded contour 40

2.29 Three types of cooling channel applied in hot stamping tool, (a.): Drilled holes (b.): Shell structure (c.): Cast-in 41

3.1 Simplified process condition from the actual hot stamping process 45

3.2 Flowchart of research methodology applied 46

3.3 3-D model of the experimental tool used in the finite element analysis and the experimental work 48

3.4 Detail dimensioning of the cooling channel used in the finite element analysis 48

3.5 3-D model of half thickness blank and the gripper in contact with blank in the analysis of heat loss during transferring. 51

3.6 Simplified 3-D model of experimental tool and the half thickness blank used in thermal analysis 53

3.7 Positioning of thermocouples for measuring the temperature install inside the tool insert 56

3.8 The experimental setup to determine the effect of applied pressure to the heat transfer coefficient 57

4.1 Illustration of heat flow from the blank to the cooling fluid in hot stamping process. 62

4.2 Illustration of heat flow within the half thickness of the blank 63

4.3 (a.): Heat flow direction inside blank (b.): The element (blank) breakdown into numbers of grid. 66

4.4 Result graph of the blank core temperature changes over time based on the numerical model. 69

4.5 Illustration of contact surface resistance and the temperature different between two surfaces. 70

5.1 Temperature distribution on the blank with transferring time at the end of five second 74

5.2 Temperature gradient at the X and Z-axis at the end of transferring time of five second. 75

5.3 Graphical presentation of temperature distribution on the blank and tool insert after 12 second with TCC of 1000 W/m² K. 77

5.4 Graph of blank and tool surface temperature change over time with TCC of 1000 W/m²K probe at thermocouple measuring location 77

5.5 Graphical presentation of temperature distribution on the blank and tool insert after 12 second with TCC of 1300 W/m² K. 78

5.6 Graph of blank and tool surface temperature change over time with TCC of 1300 W/m²K probe at thermocouple measuring location 78

5.7 Graphical presentation of temperature distribution on the blank and tool insert after 12 second with TCC of 1500 W/m² K. 79

5.8 Graph of blank and tool surface temperature change over time with TCC of 1500 W/m²K probe at thermocouple measuring location 79

5.9 Graphical presentation of temperature distribution on the blank and tool insert after 12 second with TCC of 1700 W/m² K. 80

5.10 Graph of blank and tool surface temperature change over time with TCC of 1700 W/m^2K probe at thermocouple measuring location 80

5.11 Graphical presentation of temperature distribution on the blank and tool insert after 12 second with TCC of 2000 W/m²K 81

5.12 Graph of blank and tool surface temperature change over time with TCC of 2000 W/m2K probe at thermocouple measuring location 81

5.13 Comparison of the blank temperature over time at different thermal contact conductance (W/m^2K) 82

5.14 Comparison of tool surface temperature over time at different thermal contact conductance 83

5.15 Measured blank and tool surface temperature evolved as being press inside tool at 5 MPa applied contact pressure 85

5.16 Measured blank and tool surface temperature evolved as being press inside tool at 10 MPa applied contact pressure 85

5.17 Measured blank and tool surface temperature evolved as being press inside tool at 20 MPa applied contact pressure 86

5.18 Measured blank and tool surface temperature evolved as being press inside tool at 30 MPa applied contact pressure 86

5.19 Measured blank and tool surface temperature evolved as being press inside tool at 35 MPa applied contact pressure 87

5.20 Comparison of average measured blank temperature evolve over time at different value of applied pressure 88

5.21 Comparison of average measured tool temperature evolve over time at different value of applied pressure. 89

5.22 Comparison between thermal analysis (applied thermal contact conductance h_c = 1000 W/m²K) and experiment result (applied pressure = 5 MPa) 90

5.23 Comparison between thermal analysis (applied thermal contact conductance h_c = 1300 W/m²K) and experiment result (applied pressure = 10 MPa) 91

5.24 Comparison between thermal analysis (applied thermal contact conductance h_c = 1700 W/m²K) and experiment result (applied pressure = 20 MPa) 91

5.25 Comparison between thermal analysis (applied thermal contact conductance h_c = 1700 W/m²K) and experiment result (applied 92 pressure = 30 MPa)

5.26 Comparison between thermal analysis (applied thermal contact conductance h_c = 2000 W/m²K) and experiment result (applied pressure = 35 MPa) 92

5.27 Dimensionless temperature of the blank at 5 MPa applied pressure. 94

5.28 Dimensionless temperature of the blank at 10 MPa applied pressure. 95

5.29 Dimensionless temperature of the blank at 20 MPa applied pressure. 95

5.30 Dimensionless temperature of the blank at 30 MPa applied pressure. 96

5.31 Dimensionless temperature of the blank at 35 MPa applied pressure. 96

5.32 Heat transfer coeeficient between blank (boron steel) and tool (stavax tool steel) as function of temperature of the blank 97

5.33 Influence of applied pressure to average thermal contact conductance values between the blank and tool surface. 98

5.34 Comparison of calculated maximum and the maximum thermal contact conductance value obtained by Merklein 99

5.35 Comparison of measured blank temperature curve at 5 MPa applied pressure and the FEA simulation with calculated average thermal contact conductance 100

5.36 Comparison of measured blank temperature curve at 10 MPa applied pressure and the FEA simulation with calculated average thermal contact conductance 100

5.37 Comparison of measured blank temperature curve at 20 MPa applied pressure and the FEA simulation with calculated average thermal contact conductance 101

5.38 Comparison of measured blank temperature curve at 30 MPa applied pressure and the FEA simulation with calculated average thermal contact conductance 101

5.39 Comparison of measured blank temperature curve at 35 MPa applied pressure and the FEA simulation with calculated average thermal contact conductance 102

5.40 Comparison of surface temperature evolve up to martensite formation stop temperature at different value of thermal contact conductance in FEA 103

5.41 Comparison of average tool surface temperature evolve up to martensite formation stop temperature in actual experiment. 103

5.42 Comparison of time taken by the blank cooling time achieved by FEA and actual experiment 104

5.43 Actual blank temperature evolve from exit from furnace until the blank reach a temperature of 200 ºC. 106

5.44 Comparison of blank cooling rates and hardness achieved in the actual experiment 107

LIST OF SYMBOLS

C_p	Specific Heat
k	Thermal Conductivity
Ø	Diameter
h_c	Thermal Contact Conductance Coefficient
Q	Total Heat
R_e	Reynold Number
ρ	Density
P_r	Prandalt Number
q	Heat Flux
α	Thermal Diffusivity
R_c	Thermal Contact Resistance
∞	Infinity

LIST OF ABBREVIATIONS

UHSS	Ultra-High Strength Steel
HTCS	High Thermal Conductivity Steel
CAD	Computer Aided Design
FEA	Finite Element Analysis
3-D	Three Dimensional
1-D	One Dimensional
HRC	Rockwell Hardness
MPa	Mega Pascal
KN	Kilo Newton
FCC	Face Centered Cubic
BCT	Body Centered Tetragonal
Al-Si	Aluminum Silicon
Fe	Ferum
HV	Vickers Hardness

CHAPTER 1

INTRODUCTION

1.0 CURRENT TREND

The increasing awareness of environmental pollution caused by vehicle emission has driven automotive manufacturers around the world to improve fuel efficiency by producing a lighter vehicle without compromising vehicle safety. Reducing the weight of the vehicle requires the component to have lesser or thinner material but at the same time having the same or even better mechanical properties. This has resulted in the introduction of ultra-high strength steel (UHSS) to meet the challenge.

Most UHSS as shown in figure 1.1, are made to have high mechanical properties. Although their mechanical properties are remarkably high, a major setback is in forming where high forming load is required and closely associated with short tool life and the low formability of the material. Unlike other UHSS materials, boron steel gains its final strength through the heat treatment process which alters its mechanical properties as well as increasing its hardness. In annealed condition, the yield strength of boron steels sheet (typically coated 22MnB5) are only half the strength of other UHSS but after it has been heat treated the yield strength increases up to 1200 MPa. With the capability of having an yield strength of 1200 MPa (after being hardened) the possibilities of weight reduction in automotive vehicle is enormous and in today's vehicle there are more automotive component which are related to vehicle safety such as the A-pillar, B-pillar, chassis, roof rail and many others been formed by boron steel material (Altan, 2006)(figure 1.2).

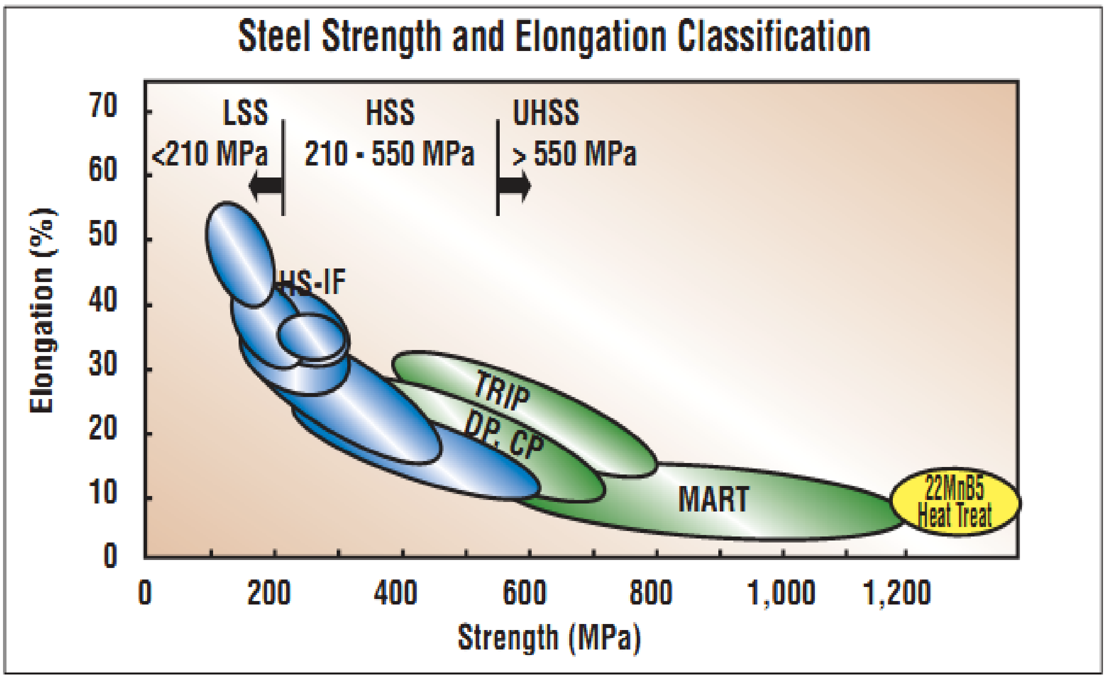

Figure 1.1: Yield strength comparison between boron steel (code name: 22MnB5) and typical sheet metal used for automotive component

(Altan, 2006)

In the heat treatment process, boron steel is heated to austenization temperature about 900 - 950 °C to induce the microstructure phase transformation. At this point, not only the microstructure phase changes from a mixture of ferrite and pearlite to austenite phase but also reduces the strength of the materials as well as increasing the elongation which are practical for the forming operation. In order to take advantage of this phenomenon, a special forming technique so called 'Hot Stamping' has been developed to suit the forming and hardening process of boron steel. In general, this technique combines the process of forming at elevated temperature and rapid cooling or queching of the blank (also made of boron steel) in a single operation tool. This specially designed stamping tool is capable of forming the blank into shape and cooling down the blank rapidly through the conduction between the blank surface in contact with liquid cooled tool surface . This technique is proven to be more effective to reduce the spring-back effect and improve the formability of material thus indirectly reducing the forming force and allowing for smaller press machine tonnage (Mori et al., 2005).

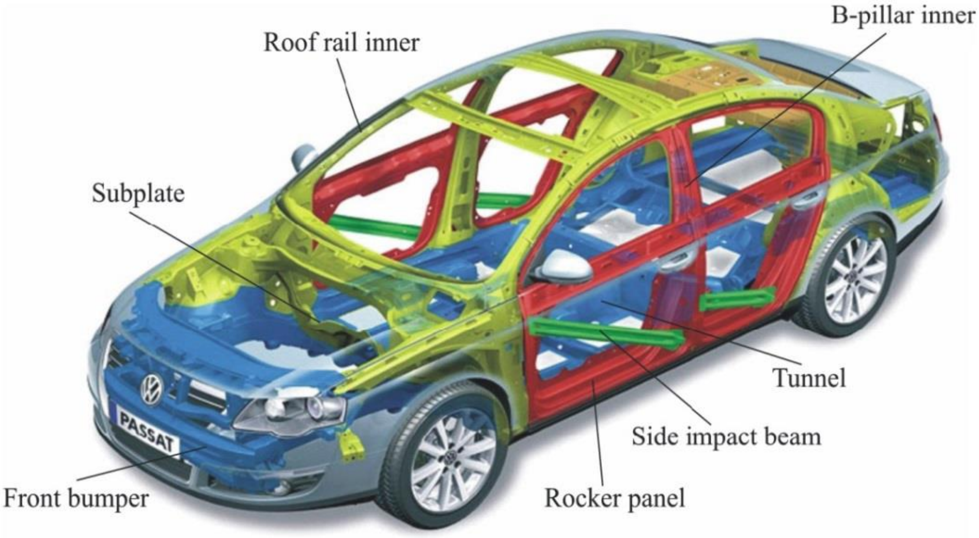

Figure 1.2: Typical vehicle component produced from 22MnB5 Boron Steel sheet

(Karbasian and Tekkaya, 2010)

1.1 HOT STAMPING

In hot stamping (figure 1.3), the pre-cut boron steel sheet is heated to the austenization temperature approximately at 900 - 950 °C for 5 to 10 minutes in a furnace to induce the microstructure phase of the blank changing to austenite microstructure. As the temperature is reached, the blank is transferred as quickly as possible to the hot stamping tool to avoid temperature drop. Then, as the tool closes the forming operation take place where the blank is formed into shape according to the contour surface of the tool. This forming operation must take place before the beginning of the martensitic transformation. Therefore, fast tool closing and forming are the preconditions for a successful process. As the tool reaches the bottom end stroke, it will dwell for a certain time (depending on the blank size) to allow the quenching operation to take place. At this stage the blank needs to be cooled down through conduction to the tool surface with minimum cooling rate of 30 ºC per second to force the microstructure phase transformation of the boron steel blank from austenitic phase to fully martensitic phase thus giving the high final part strength or otherwise the final yield strength of

1200 MPa might not be achieved (Abdul Hay et al., 2010). Soon after that, the tool is opened to remove the formed blank, ready for the next operation.

A successful process control can be defined by two main criteria; the ability to form the blank into shapes as well the ability to hardened the blank so that the final part would have yield strength of 1200 MPa and ultimate tensile strength at 1500 MPa. In the process, forming the blank at high temperature is not a major issue since the process of heating itself improves the formability of the blank but for hardening the blank, a few parameters such as cooling rate, initial tool temperature, applied pressure and so on need to be carefully considered. A slow cooling rate would cause the formation of bainite microstructure phase instead of martensite (figure 1.4) which affects the final part strength while fast cooling rates would increase the cost of lowering the tool temperature to accelerate the blank cooling rate (Chang et al., 2011). So an experimental studies need to be done to investigate the optimal process parameters such as applied pressure to the blank, initial tool temperature and the cooling rate of the the blank.

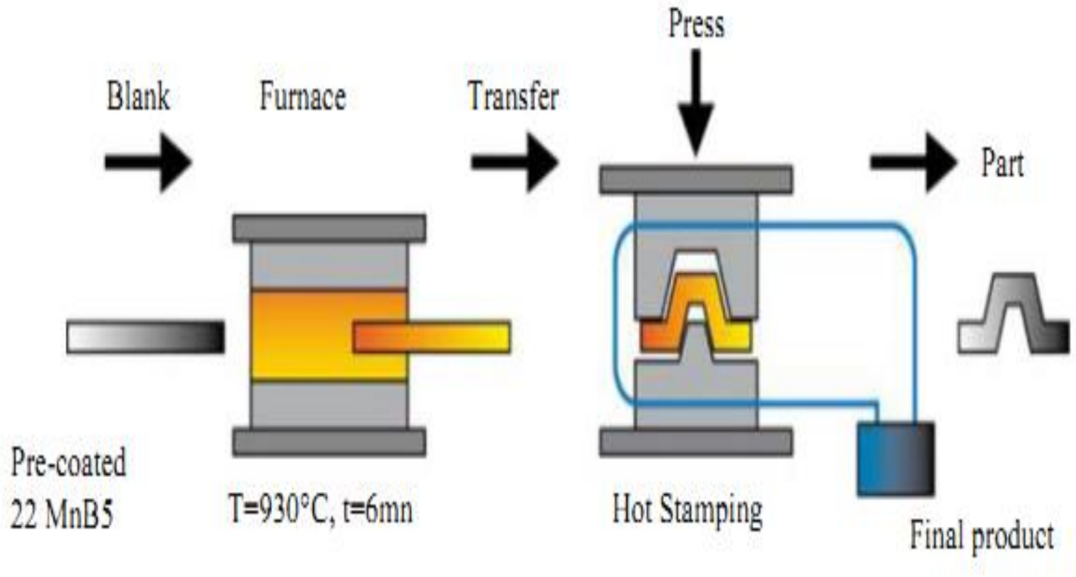

Figure 1.3: Typical process flow of hot stamping process

(Abdul Hay et al., 2010)

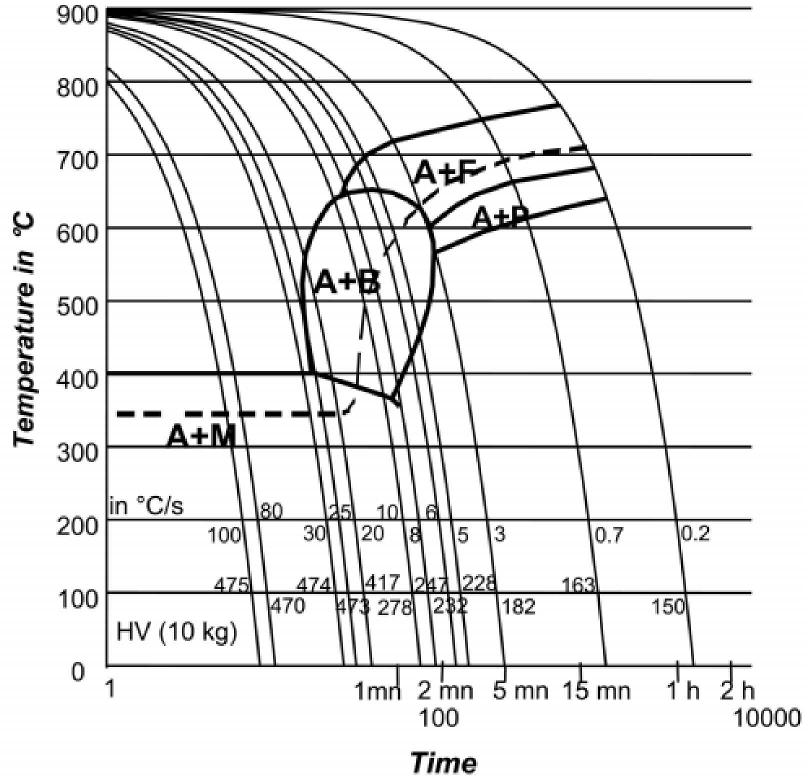

Figure 1.4: Continuous cooling transformation diagram of 22MnB5 boron steel.

(Naganathan, 2010)

1.2 PROBLEM STATEMENT

In hot stamping,one of the key factors for successful production of the stamped part with a ultimate strength of 1500 MPa is the ability to control the cooling rate of the blank during the quenching inside the forming tool. The blank needs to be cooled down at a rate of less than 30 ºC/s in order to fully transform the austenite phase to martensitic microstructure phase(Karbasian and Tekkaya, 2010). During the process, the quenching needs to be performed as the forming operation is completed where the tool dwells for a few second at the bottom stroke. As the tool dwells, the formed blank is fully in contact with the tool surface consequently conducting the heat from the blank to the tool materials and rapidly cooling down the blank. At this point, process parameters such as applied contact pressure and initial tool temperature as well as the tool material play an important role in controlling the blank cooling rate. A tool material with a higher thermal conductivity is capable of conducting the heat faster, while higher applied pressure reduces the heat resistance at the contact interface. A lower tool temperature accelerates the blank cooling rate thus shortening the part cycle time(Karbasian and Tekkaya, 2010). So, based on these criteria most tool makers prefer high thermal conductivity tool steel (HTCS) as the material for the tool insert and during the process, the tool temperature is maintained at 5 - 10 °C. Despite the advantage of high thermal conductivity and low tool temperature, the drawback is the high tool cost and the operational cost is very high. The price of HTCS is almost triple the price of hot tool steel and this is further complicated by the lack of steel makers in this region. As a result the material cost is increased due to transportation as well as increasing the procurement lead time. In addition in equatorial climates, maintaining low tool temperature using chilled water requires high energy utilization thus raising the operational cost. Also very low tool temperature leads to condensation on the tool surface due to high humidity which could accelerate corrosion. An alternative to the situation, HTCS materials could be replace with low thermal conductivity steel as the tool materials and the initial tool temperature set just slightly lower than ambient temperature (20 – 25 ºC) capable to reduce the transportation and the lower the energy consumption for chilled water but in another hand increase the process cycle time. Thus, a study on the tool material and the process parameters needs to be done to optimize the process.

1.3 RESEARCH OBJECTIVES

This research has the following objectives:

(i) To conduct a thermal analysis simulation of the actual experimental process.

(ii) To design and fabricate an experimental setup to evaluate the thermal contact conductance between the boron steel blank and the tool .

(iii) To determine the influence of applied pressure, P on the thermal contact conductance, h_c at the interface between the blank (boron steel material) and tool material (STAVAX Tool Steel).